

RESEARCH

Open Access



Hydrogen sulfide activates calcium signaling to confer tolerance against selenium stress in *Brassica rapa*

Xiefeng Ye^{1†}, Haiyan Lu^{2†}, Aijing Xin³, Ruixian Liu⁴, Zhiqi Shi², Jian Chen^{2*}  and Lifei Yang^{3*}

Abstract

Background Se (selenium) pollution is an emerging environmental concern. Excessive Se induces phytotoxicity. The endogenous H₂S (hydrogen sulfide) was involved in plant adaptation to Se stress, but the signaling player of H₂S remains unclear.

Methods The study was conducted in a hydroponic system with different chemicals added to the treatment solution. Fluorescent tracking was performed to detect endogenous signaling molecules in plant tissues. Physiological changes were determined based on pharmacetics and histochemical experiments. Gene expression was analyzed using qRT-PCR. The data were summarized using hierarchical cluster and Pearson correlation analysis.

Results Se stress inhibited *B. rapa* growth (e.g. root elongation, shoot height, and seedling fresh weight and dry weight) in both dose- and time-dependent manners, with approximately 50% of root growth inhibition occurred at 20 μM Se. Se stress induced ROS (reactive oxygen species) accumulation and oxidative injury in *B. rapa*. Se exposure resulted in the upregulation of *LCDs* (*L-cysteine desulfhydrase*) and *DCDs* (*D-cysteine desulfhydrase*) encoding enzymes for H₂S production in *B. rapa* at early stage of Se exposure, followed by downregulation of these genes at late stage. This was consistent with the change of endogenous H₂S in *B. rapa*. Enhancing endogenous H₂S level with NaHS (H₂S donor) stimulates endogenous Ca²⁺ in *B. rapa* upon Se exposure, accompanied the attenuation of growth inhibition, ROS accumulation, oxidative injury, and cell death. The beneficial effects of H₂S on detoxifying Se were blocked by decreasing endogenous Ca²⁺ level with Ca²⁺ channel blocker or Ca²⁺ chelator. Finally, hierarchical cluster combined with correlation analysis revealed that Ca²⁺ might acted as downstream of H₂S to confer Se tolerance in *B. rapa*.

Conclusion Ca²⁺ was an important player of H₂S in the regulation of plant physiological response upon Se stress. Such findings extend our knowledge of the mechanism for Se-induced phytotoxicity.

Keywords *Brassica rapa*, Calcium, Hydrogen sulfide, Phytotoxicity, Reactive oxygen species, Selenium stress

[†]Xiefeng Ye and Haiyan Lu contributed equally to this work.

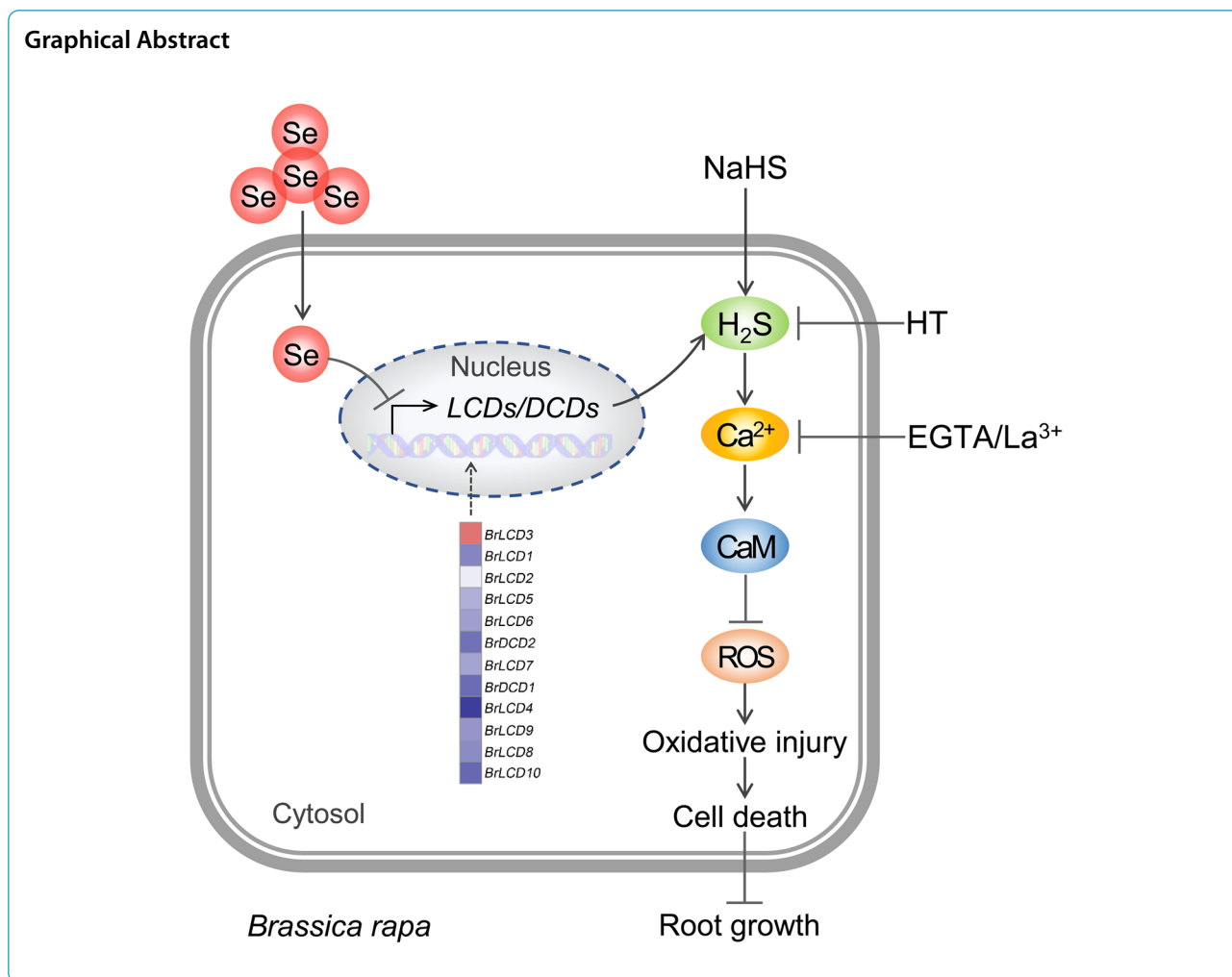
*Correspondence:

Jian Chen
chenjian@jaas.ac.cn
Lifei Yang
lfy@njau.edu.cn

Full list of author information is available at the end of the article



© The Author(s) 2024. **Open Access** This article is licensed under a Creative Commons Attribution 4.0 International License, which permits use, sharing, adaptation, distribution and reproduction in any medium or format, as long as you give appropriate credit to the original author(s) and the source, provide a link to the Creative Commons licence, and indicate if changes were made. The images or other third party material in this article are included in the article's Creative Commons licence, unless indicated otherwise in a credit line to the material. If material is not included in the article's Creative Commons licence and your intended use is not permitted by statutory regulation or exceeds the permitted use, you will need to obtain permission directly from the copyright holder. To view a copy of this licence, visit <http://creativecommons.org/licenses/by/4.0/>.



Introduction

Se (selenium) contamination has been becoming an emerging environmental concern due to agricultural and industrial activities (He et al. 2018). Se is an essential nutrient for mammals. Mammals take up Se mainly through consuming agro-products containing Se. Therefore, food crops with Se biofortification has been becoming popular, requiring the increase in the application of Se-enriched fertilizers in agricultural environment (Sarwar et al. 2020). Excessive use of these fertilizers increases Se level in soil, sediments, and groundwater (Bajaj et al. 2011; Mehdi et al. 2013; Winkel et al. 2012). Mining industries (such as metals, phosphate, and coal mining) also accelerate the release of Se into the environment (Etteieb et al. 2020). Excessive Se leads to serious environmental pollution (Sakamoto et al. 2012). The limit of 10 µg/L has been commonly used for Se in drinking water in most countries (Vinceti et al. 2013). In some regions, the concentration of Se in water is up to 669.5–1400 µg/L (Bajaj et al. 2011; Kuisi & Abdel-Fattah 2010;

Zelmanov & Semiat 2013). Irrigation of Se-rich soil can accelerate the mobilization of Se to enlarge the pollution (Kausch & Pallud 2013).

Se at low level is beneficial for plants' adaptation to stress conditions, but excessive Se inhibits plant growth by inducing physiological disorders. Se-induced phytotoxicity depends on different Se forms and different plant species. In plants, SeO₃²⁻ is more toxic than SeO₄²⁻ because SeO₃²⁻ is easier to be incorporated into the Se-amino acids in plant cells. This process causes protein dysfunction, further resulting in phytotoxicity and growth inhibition (Lyons et al. 2005). SeO₃²⁻ at 50–100 µM remarkably inhibits the biomass of pea, maize, Indica mustard, and *Arabidopsis* (Hawrylak-Nowak 2008; Lehotai et al. 2016; Molnár et al. 2018). Some plant species are even more sensitive to Se stress. SeO₃²⁻ at more than 20 µM reduces the growth and productivity of cucumber and lettuce (Hawrylak-Nowak 2013; Hawrylak-Nowak et al. 2015). Se-induced phytotoxicity includes oxidative injury, nutrient deficiency,

and phytohormones disturbance, etc. (Hasanuzzaman et al. 2020b). Oxidative stress is one of the typical consequences of Se-induced phytotoxicity. Se stress inhibits root growth by disturbing the homeostasis of ROS (reactive oxygen species) and RNS (reactive nitrogen species) in *Arabidopsis thaliana* (Kolbert et al. 2016). Se-induced increase in ROS content and lipid peroxidation have been found in variable plant species, such as *Pisum sativum* (Lehotai et al. 2016), *Brassica rapa* (Chen et al. 2014a), *Triticum aestivum* (Łabanowska et al. 2012), and *Hordeum vulgare* (Akbulut & Cakir 2010). The protective role of Se in plants have been extensively studied in detail, but Se-induced phytotoxicity has not been fully understood.

The endogenous gaseotransmitter H₂S (hydrogen sulfide) plays vital roles in regulating plant growth and development. In plant cells, H₂S can be generated by LCD (_L-cysteine desulphydrase, EC4.4.1.1) and DCD (_D-cysteine desulphydrase, EC4.4.1.15) (Arif et al. 2021). H₂S has been characterized as a defensive signaling molecule combating stress conditions (Zhang et al. 2021). Our previous study demonstrated that Se stress inhibited the root growth of *Brassica rapa* (Chinese cabbage) by suppressing endogenous H₂S (Chen et al. 2014b), while other players related to H₂S signal pathway are still missing in plants upon Se stress. H₂S can interact with various signaling molecules to regulate plant intrinsic physiology (Wang et al. 2021a). Ca²⁺ is one of the important player of H₂S. Ca²⁺ is an important second messenger for plant stress adaptation (Tong et al. 2021). Ca²⁺ can act both upstream and downstream of H₂S in plants in response to variable abiotic stimuli (Li 2019). CaM (calmodulin), one of the core transducers of Ca²⁺ signaling, is also involved in the interplay between H₂S and Ca²⁺ (Fang et al. 2014). However, it is unclear whether and how H₂S-Ca²⁺ interaction regulates Se-induced phytotoxicity.

In this work, we analyzed Se stress-inhibited growth of *B. rapa* seedlings. The role of H₂S-Ca²⁺ interaction in the regulation of *B. rapa* tolerance against Se stress was studied. The results of this work may help understand the mechanism for plant physiological adaptation to Se stress.

Materials and methods

Plant culture and treatment

The seeds of *B. rapa* were sterilized with NaClO (1%) for 5 min, followed by washing with distilled water and germinating at 25 °C for 24 h. Then the germinated seeds were transferred to a floating net, culturing with 1/4 strength Hoagland solution in a light chamber with active radiation of 200 μmol/(m² s), photoperiod of 12 h, and temperature at 25 °C, based on our previous study (Cheng et al. 2021). About 30 seedlings with

root length at 1.5 cm were cultured at 700 mL nutrient solution with Na₂SeO₃ added at different concentration (0–80 μM). Various chemicals were added to the nutrient solution for different treatment. NaHS (10 μM) and HT (hypotaourine) (20 μM) were applied as H₂S donor and H₂S scavenger, respectively. EGTA (ethylene glycol-bis(2-aminoethylether)-N,N,N',N'-tetraacetic acid) (0.5 mM) and LaCl₃ (50 μM) were applied as Ca²⁺ chelator and Ca²⁺ channel blocker, respectively (Li et al. 2014). Plant tissues were harvested after treatment, respectively, followed by physiological measurement.

Fluorescent detection

We used several specific fluorescent probes to perform histochemical detection in situ in roots based on our previously published methods (Li et al. 2014; Yang et al. 2022). Endogenous H₂S, Ca²⁺, total ROS, cell death were detected by using WSP-1 (Washington State Probe-1), Fluo-3, DCFH-DA (2',7'-dichlorofluorescein diacetate), and PI (propidium iodide), respectively. WSP-1 was obtained from Beijing Solarbio Science & Technology Co., Ltd (Beijing, China). Fluo-3, DCFH-DA, and PI were obtained from Beyotime Biotech. Inc (Shanghai, China). The fluorescent images were captured with a fluorescence microscope (ECLIPSE, TE2000-S, Nikon, Melville, NY, USA). Image-Pro Plus 6.0 (Media Cybernetics, Inc., Rockville, MD, USA) was applied to calculate relative fluorescent density for each image.

Histochemical detection

Endogenous hydrogen peroxide and superoxide radical in leaves were detected in vivo by using DAB (3,3-diaminobenzidine) and NBT (nitro-blue tetrazolium) staining, respectively (Zhou et al. 2008). For hydrogen peroxide detection, leaves were incubated in DAB (0.1 w/v, pH 3.8) at 25 °C for 30 min. For superoxide radical detection, leaves were incubated in 6 mM NBT (dissolved in 10 mM sodium-citrate buffer, pH 6.0) at 25 °C for 30 min. The leaves with specific staining were transferred to boiling ethanol for 30 min to remove the green background (chlorophyll), followed by photographed with a digital camera.

The lipid peroxidation in root was histochemically detected by using Schiff's reagent. The roots were stained in Schiff's reagent for 15 min, followed by washing with K₂S₂O₅ solution (0.5% w/v in 0.05 M HCl) for 10 min. The loss of membrane integrity in roots were histochemically detected using Evans blue. The roots were incubated at Evans blue solution (0.025%, w/v) for 15 min, followed by washing with distilled water for 10 min. For the histochemical detection in leaves, the leaves were stained with the reagent as described above. Then the stained leaves

were incubated in boiling ethanol for 30 min to remove chlorophyll, followed by photographed with a digital camera (Ye et al. 2016).

Gene expression analysis

We selected Trizol (Invitrogen, ThermoFisher Scientific, Shanghai, China) to extract total RNA from plant tissues based on manufacturer's instructions. The reaction mixture for reverse transcription consisted of M-MLV (200 units), RNAase inhibitor (20 units), ligo (dT) primers (0.5 μ g), and RNA (3 μ g). The obtained first cDNA was used as template to perform quantitative RT-PCR using Applied Biosystems 7500 Fast Real-Time PCR System (LifeTechnologies™, ThermoFisher Scientific, Shanghai, China). The abundance of gene expression was quantified using $2^{-\Delta\Delta T}$ threshold cycle method (Livak & Schmittgen 2001). The relative abundance of *Actin* was applied as internal standard to standardize the results. The primers used for amplifying target genes were listed in Table S1.

Data analysis

Each result were shown as mean \pm SD (standard deviation) with at least three replicates. The significant difference between two designated data sets was evaluated by ANOVA (one-way analysis of variance) combined with F-test at $P < 0.05$. LSD (least significant difference) was performed to make multiple comparison analysis at $P < 0.05$. The package "corrplot" in R was used to perform Pearson correlation analysis among different parameters. The heatmaps for hierarchical cluster analysis and gene

expression analysis were generated by using the package "pheatmap" in R and TBtools (Chen et al. 2020).

Results

Se stress inhibited the growth of *B. rapa*

We analyzed the phenotype of *B. rapa* seedlings under different concentrations of SeO_3^{2-} (0–80 μ M) up to 72 h. Se stress inhibited the seedling growth in a dose-dependent manner (Fig. 1A, B). The root length significantly decreased by 5.83%, 23.2%, 50.4%, 60.5%, and 76.8% at 5, 10, 20, 40, and 80 μ M Se, respectively, as compared to control (Fig. 1C). The shoot height significantly decreased by 12.8%, 25.1%, 34.9%, 42.1%, and 48.2% at 5, 10, 20, 40, and 80 μ M Se, respectively, as compared to control (Fig. 1D). The FW (fresh weight) of seedlings significantly decreased by 14.7%, 20.6%, 35.3%, 58.5%, and 73.5% at 5, 10, 20, 40, and 80 μ M Se, respectively, as compared to control (Fig. 1E). The DW (dry weight) of seedlings were significantly inhibited by Se at high concentrations (40–80 μ M) (Fig. 1F), which may be resulted from the decrease in RWC (relative water content) (Fig. 1G).

As the root length under 20 μ M Se treatment was about half of control, we monitored the time-course changes of seedling growth upon 20 μ M Se. Compared to the control, Se treatment began to significantly prohibit root elongation after exposure of 12 h, followed by decreased growth speed of root with the prolong of treatment time (Fig. 2A). The root FW showed similar changes with root length upon Se exposure (Fig. 2B). The shoot FW and whole plant FW were decreased after 24 h of 20 μ M Se treatment (Fig. 2C, D).

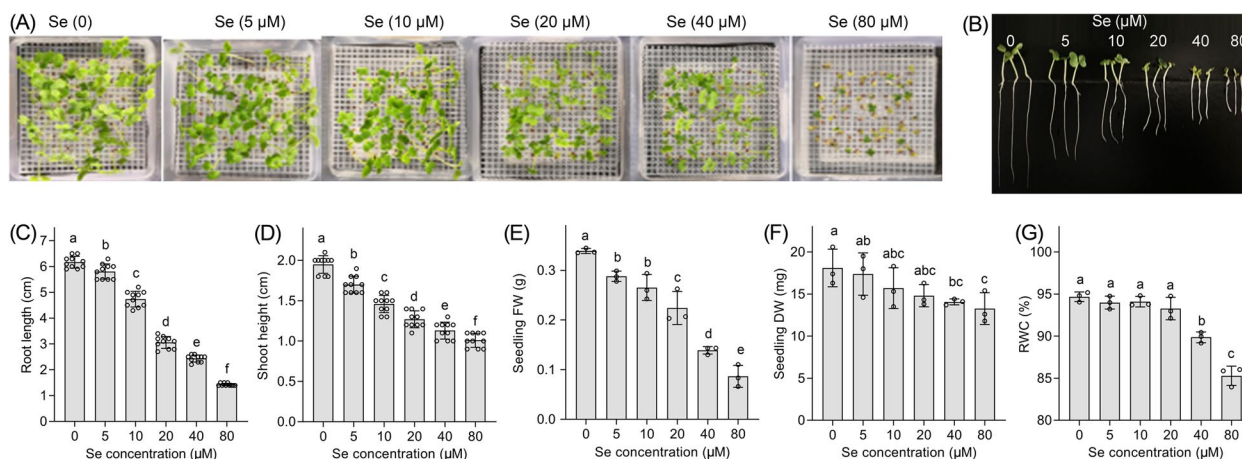


Fig. 1 Growth changes of *B. rapa* seedlings upon Se exposure. **A** Photos of seedlings grown in hydroponics with different concentrations of Se for 72 h. **B** Phenotype of seedlings after treated with Se for 72 h. Bar = 1 cm. **C** The root length of seedlings. **D** The shoot height of seedlings. **E** The fresh weight of seedlings. **F** The dry weight of seedlings. **G** The RWC of seedlings. Different lowercase letters in (C–G) indicated significant difference among different treatments ($n = 3–10$; $P < 0.05$; LSD, ANOVA)

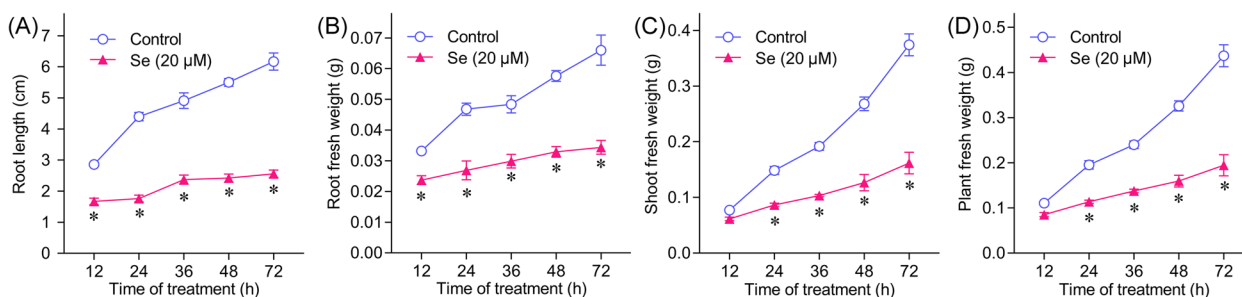


Fig. 2 Time-course observation of the growth of *B. rapa* seedlings under 20 μM Se. **A** Root length. **B** Root fresh weight. **C** Shoot fresh weight. **D** Whole plant fresh weight. Asterisk indicated significant difference between control and treatment of 20 μM Se at each time point ($n=3-10$; $P<0.05$; ANOVA)

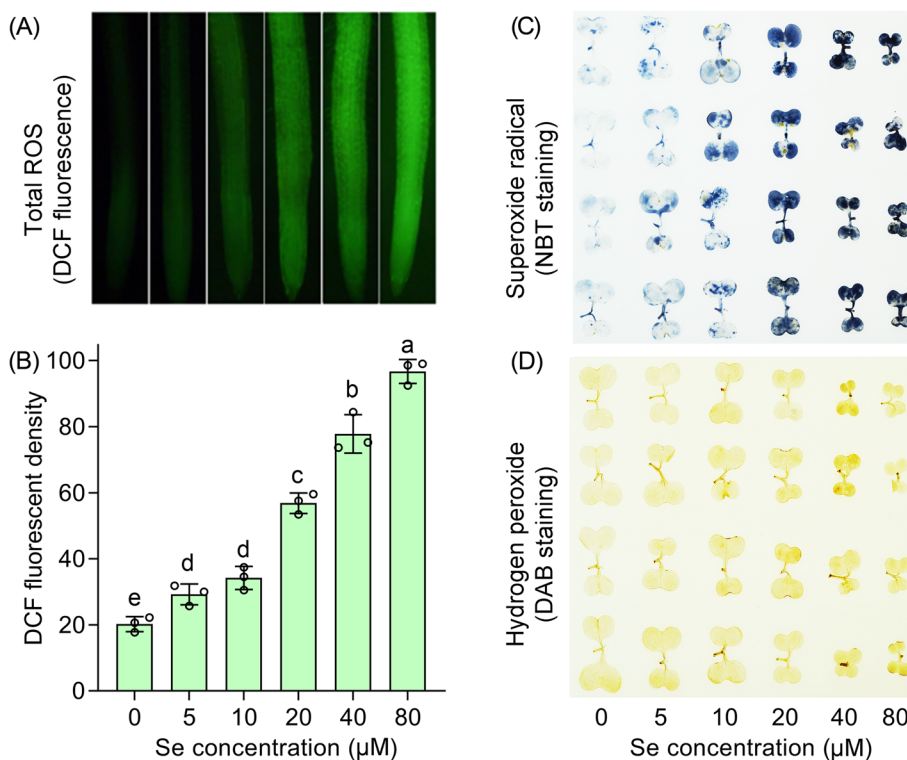


Fig. 3 ROS accumulation in *B. rapa* seedlings under Se stress. **A** Total ROS in roots indicated by DCF fluorescence. **B** DCF fluorescent density in roots. Different lowercase letters in indicated significant difference among different treatments ($n=3$; $P<0.05$; LSD). **C** Superoxide radical in leaves indicated by NBT staining. **D** Hydrogen peroxide in leaves indicated by DAB staining

Se stress induced oxidative stress in *B. rapa*

We detected total ROS level in roots using specific fluorescent probe DCFH-DA. Se stress led to ROS accumulation in roots in a dose-dependent manner (Fig. 3A). Compared to the control, the DCF fluorescent density significantly increased by 44.5%, 69.3%, 181.2%, 284.6%, and 377.7% at 5, 10, 20, 40, and 80 μM Se, respectively (Fig. 3B). In leaves, we evaluated two typical ROS

(superoxide radical and hydrogen peroxide) in vivo by using histochemical analysis. The leaves showed intensified staining with the increase in Se concentration (Fig. 3C, D), indicating that Se treatment resulted in the accumulation of superoxide radical and hydrogen peroxide in leaves.

As over-accumulated ROS always attack protein and lipid to cause oxidative stress, lipid peroxidation and loss

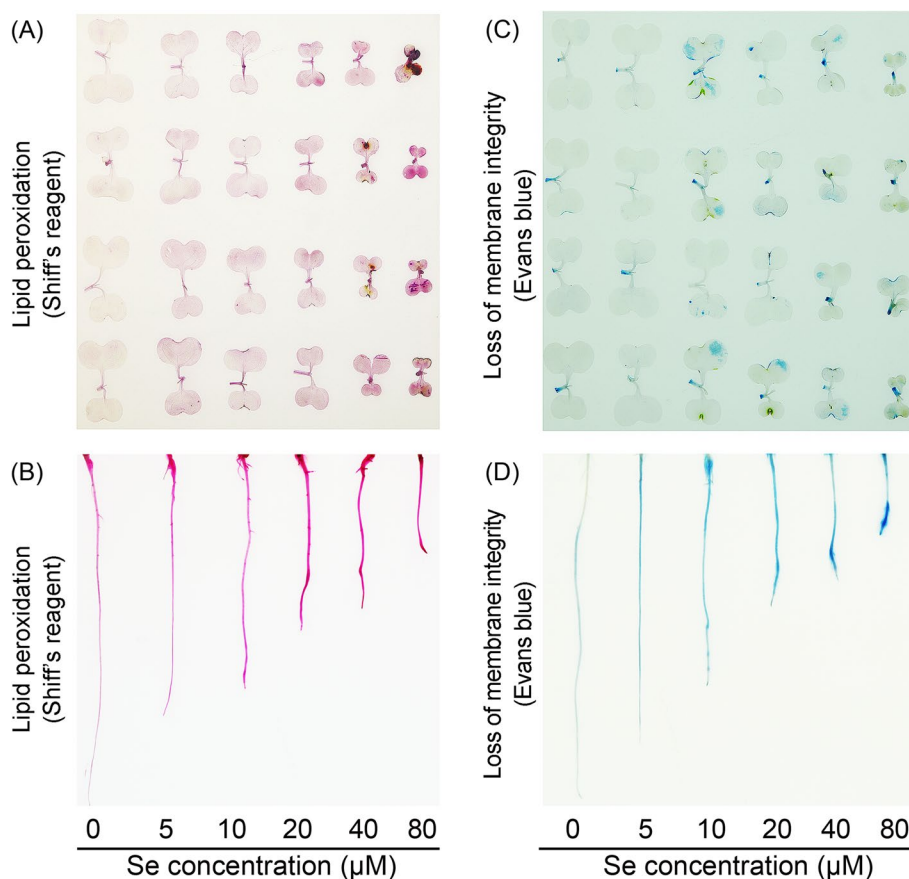


Fig. 4 Oxidative injury in *B. rapa* seedlings under Se stress. **A** Lipid peroxidation in leaves indicated by Schiff's reagent. **B** Lipid peroxidation in roots indicated by Schiff's reagent. **C** Loss of membrane integrity in leaves indicated by Evans blue. **D** Loss of membrane integrity in roots indicated by Evans blue

of membrane integrity were detected histochemically to evaluate oxidative injury in *B. rapa* seedlings upon Se exposure. We observed aggravated lipid peroxidation in both leaves and roots with the increase in Se concentration (Fig. 4A, B). Se stress also induced the loss of membrane integrity in leaves and roots (Fig. 4C, D). The roots showed more severe oxidative injury than that of leaves because of direct Se exposure of roots. These results suggested that Se stress induced oxidative injury in *B. rapa*.

Se stress disturbed endogenous H₂S level in *B. rapa*

We previously identified the gene family of *BrLCD* and *BrDCD* from the genome of *B. rapa*, which included 10 *BrLCDs* and 2 *BrDCDs* (Chen et al. 2014b). Here we detected the expression file of these genes in roots upon the exposure of Se at 20 μM that led to moderate inhibition of root elongation. Se stress induced the upregulation of most of these genes after treatment for 3–48 h followed by downregulation with prolonged treatment (72 h) (Fig. 5).

As 20 μM Se induced strong upregulation and down-regulation of H₂S-producing genes at 48 and 72 h, respectively (Fig. 5), we detected endogenous H₂S level in roots with specific fluorescent probe WSP-1 at these two time points. Se treatment for 48 h resulted in significant increase in H₂S level as compared to control, with remarkably decreased H₂S level at 72 h (Fig. 6A, B). This was consistent with the expression pattern of *BrLCDs* and *BrDCDs*. Endogenous H₂S was decreased at the end of Se treatment (72 h). H₂S was supplied by adding NaHS (H₂S donor) in the treatment solution. As expected, adding NaHS significantly enhanced endogenous H₂S level in Se-treated roots, accompanied the recovery of root elongation. The effect of NaHS was counteracted by adding H₂S scavenger HT (Fig. 6C, D). These results suggested that H₂S generation in roots was triggered upon the early exposure of Se. However, prolonged Se stress decreased H₂S generation, which was associated with the final inhibition of root growth.

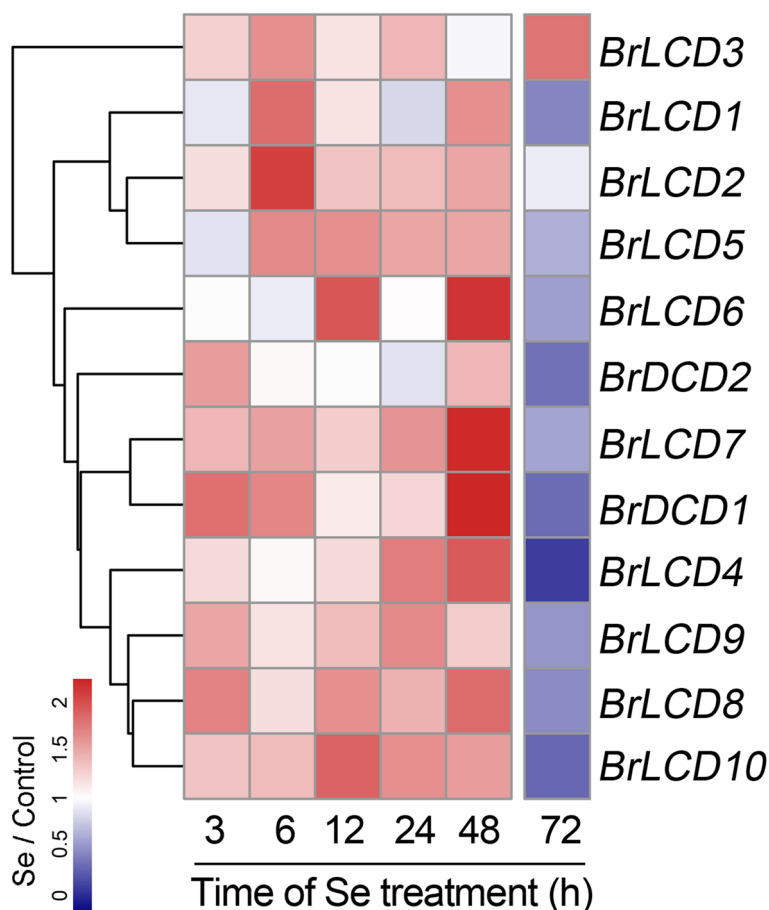


Fig. 5 Relative expression of *BrLCDs* and *BrDCDs* in the roots of *B. rapa* seedlings upon treatment of 20 μM Se. The heatmap data were shown as the expression of Se treatment with respect to control. Red, white, and blue indicated upregulation, unchanged, and downregulation, respectively

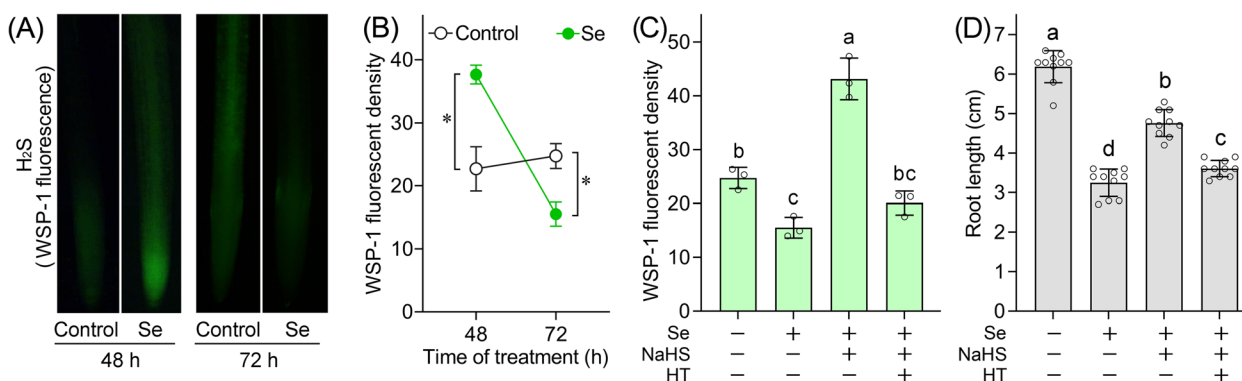


Fig. 6 The change of endogenous H_2S in the roots of *B. rapa* upon Se and NaHS. **A** Root endogenous H_2S fluorescence detected by WSP-1 upon Se (20 μM) exposure at 48 h and 72 h. **B** Calculated WSP-1 fluorescent density according to **(A)**. **C** WSP-1-based endogenous H_2S level in roots under treatment of Se (20 μM), NaHS (10 μM), and HT (20 μM) for 72 h. **D** Root length under treatment of Se (20 μM), NaHS (10 μM), and HT (20 μM) for 72 h. Asterisk in **(B)** indicated significant difference between control and Se treatment ($n=3$; $P<0.05$; ANOVA). Different lowercase letters in **(C)** and **(D)** indicated significant difference among different treatments ($n=3-10$; $P<0.05$; LSD)

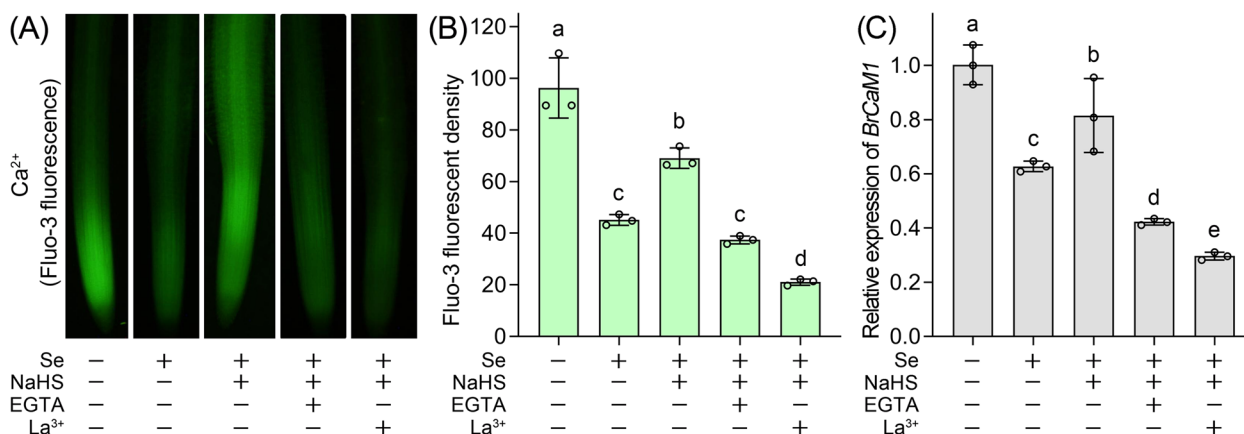


Fig. 7 H₂S activated endogenous Ca²⁺ signaling in the roots of *B. rapa* upon Se and NaHS. **A** Root endogenous Ca²⁺ fluorescence detected by Fluo-3 upon NaHS, EGTA (0.5 mM), or La³⁺ (50 μM) in the presence of Se (20 μM) for 72 h. **B** Calculated Fluo-3 fluorescent density. **C** Relative expression level of *BrCaM1* upon the same treatment. Different lowercase letters in (B) and (C) indicated significant difference among different treatments (n = 3; P < 0.05; LSD)

Ca²⁺ was involved in H₂S-regulated growth of *B. rapa* upon Se stress

We selected specific fluorescent probe Fluo-3 to detect endogenous Ca²⁺ in the roots (Fig. 7A). Se (20 μM) exposure for 72 h significantly decreased endogenous Ca²⁺ in the roots compared to control. Adding NaHS significantly enhanced endogenous Ca²⁺ in Se-treated roots, an effect reversed by further adding Ca²⁺ chelator (EGTA) or Ca²⁺ influx channel blocker (La³⁺) (Fig. 7B). The change of relative expression of *BrCaM1* showed similar pattern with endogenous Ca²⁺ upon the same treatment (Fig. 7C).

Then we detected the growth response of *B. rapa* seedlings upon the same treatment. NaHS attenuated root growth inhibition was counteracted by adding EGTA or La³⁺ under Se exposure (Fig. 8A). The fresh weight of root, shoot, and the whole seedlings also showed similar changing patterns with root length (Fig. 8B-D). The

above results suggested that H₂S activated intracellular Ca²⁺ signal to facilitate *B. rapa* growth under Se stress.

Ca²⁺ was involved in H₂S-attenuated oxidative injury in *B. rapa* upon Se stress

NaHS prohibited Se-induced ROS accumulation in roots and leaves, which could be reversed by further adding EGTA or La³⁺ (Fig. 9). NaHS attenuated Se-induced oxidative injury in roots and leaves, an effect that could be diminished by further adding EGTA or La³⁺ (Fig. 10A-D). Root cell death was detected by using Trypan blue staining and PI fluorescence, respectively. NaHS attenuated Se-induced root cell death, which could be reversed by further applying EGTA or La³⁺ (Fig. 10E-G). These results suggested that Ca²⁺ acted downstream of H₂S to ameliorate ROS accumulation, oxidative injury, and cell death in *B. rapa* upon Se stress.

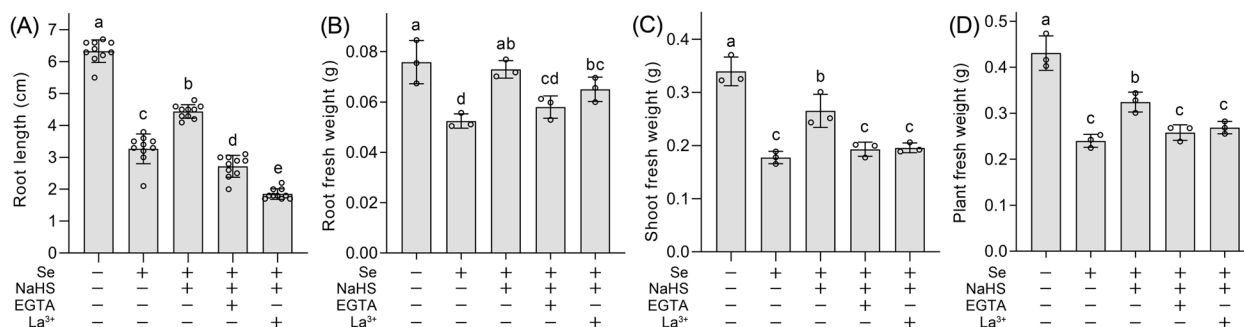


Fig. 8 H₂S-Ca²⁺ interaction promoted the growth of *B. rapa* upon Se stress. **A** Root length upon NaHS, EGTA (0.5 mM), or La³⁺ (50 μM) in the presence of Se (20 μM) for 72 h. **B** Root fresh weight. **C** Shoot fresh weight. **D** Seedling fresh weight. Different lowercase letters indicated significant difference among different treatments (n = 3–10; P < 0.05; LSD)

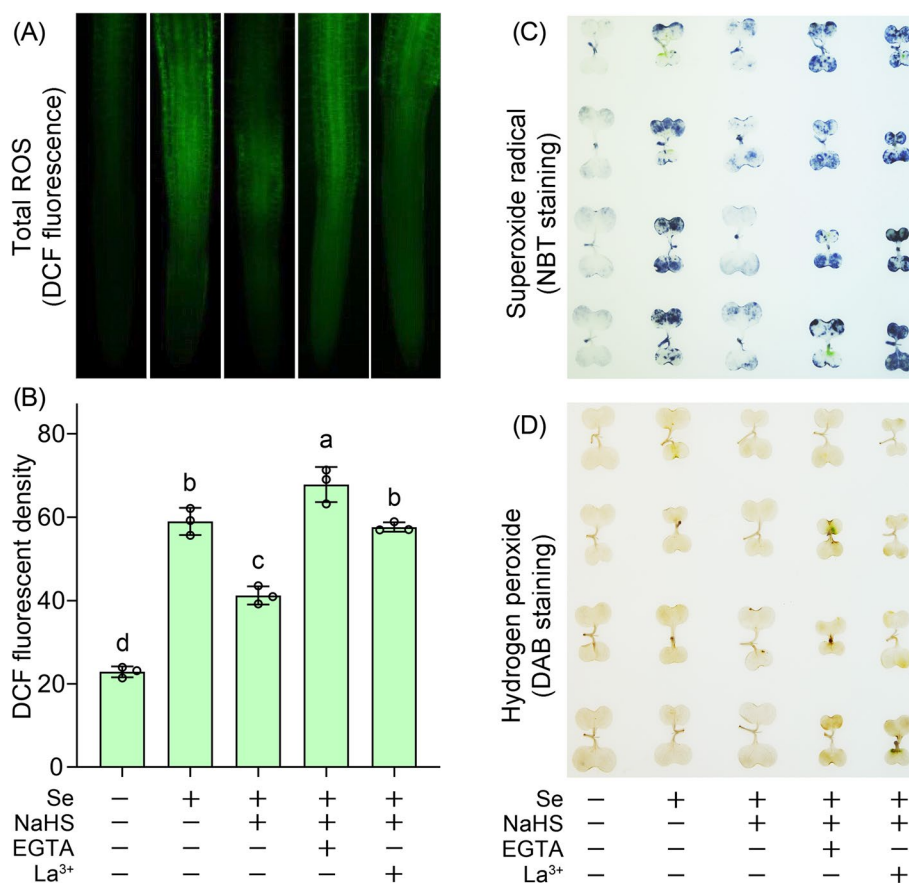


Fig. 9 H_2S - Ca^{2+} interaction prohibited ROS accumulation *B. rapa* upon Se stress. **A** Root total ROS fluorescence detected by DCF upon NaHS, EGTA (0.5 mM), or La^{3+} (50 μM) in the presence of Se (20 μM) for 72 h. **B** Calculated DCF fluorescent density. **C** NBT-stained superoxide radical in leaves upon the same treatment. **D** DAB-stained hydrogen peroxide in leaves upon the same treatment. Different lowercase letters in B indicated significant difference among different treatments ($n=3$; $P<0.05$; LSD)

Cluster analysis of H_2S - Ca^{2+} interaction in *B. rapa* upon Se stress

We performed hierarchical cluster analysis to summarize the relationship among different treatments based on the changes of physiological parameters obtained above (Fig. 11A). The control and Se+NaHS were clustered together, suggesting that NaHS was able to counteract the effect of Se. The Se+NaHS+ La^{3+} , Se+NaHS+EGTA, and Se were clustered together, suggesting that either La^{3+} or EGTA partially diminished the effect of NaHS under Se stress. Therefore, enhancing H_2S level (provided by NaHS) mitigated Se-induced physiological disorders, an effect that was partially blocked by decreasing intracellular Ca^{2+} (by adding La^{3+} or EGTA).

Then we performed Pearson correlation analysis to investigate the relationship among different physiological parameters under same treatment setup (control, Se, Se+NaHS, Se+NaHS+EGTA, and Se+NaHS+ La^{3+}) (Fig. 11B). ROS was positively correlated to cell death, indicating that ROS accumulation caused cell death in *B.*

rapa under Se stress. The growth parameters (e.g. root FW, shoot FW, total FW, and root length) were negatively correlated to ROS and cell death, respectively, indicating that ROS-triggered cell death caused growth inhibition. Ca^{2+} was positively correlated to *CaM*, suggesting the synchronous activation of Ca^{2+} signaling by H_2S . Ca^{2+} and *CaM* were positively correlated to growth parameters but negatively correlated to ROS and cell death. This indicated that H_2S activated Ca^{2+} signaling to suppress ROS and cell death in order to promote growth under Se stress.

Discussion

Se is an emerging environmental pollutant impeding plant growth. Se can cause phytotoxicity at a wide range of concentration (15–100 μM), which depends on plant species (Hasanuzzaman et al. 2020b). Se at 0.21–4.08 mg/kg (about 2.66–51.7 μM) in agricultural soil resulted in the toxic accumulation of Se in paddy rice and Chinese cabbage (Huang et al. 2009). We found that Se at

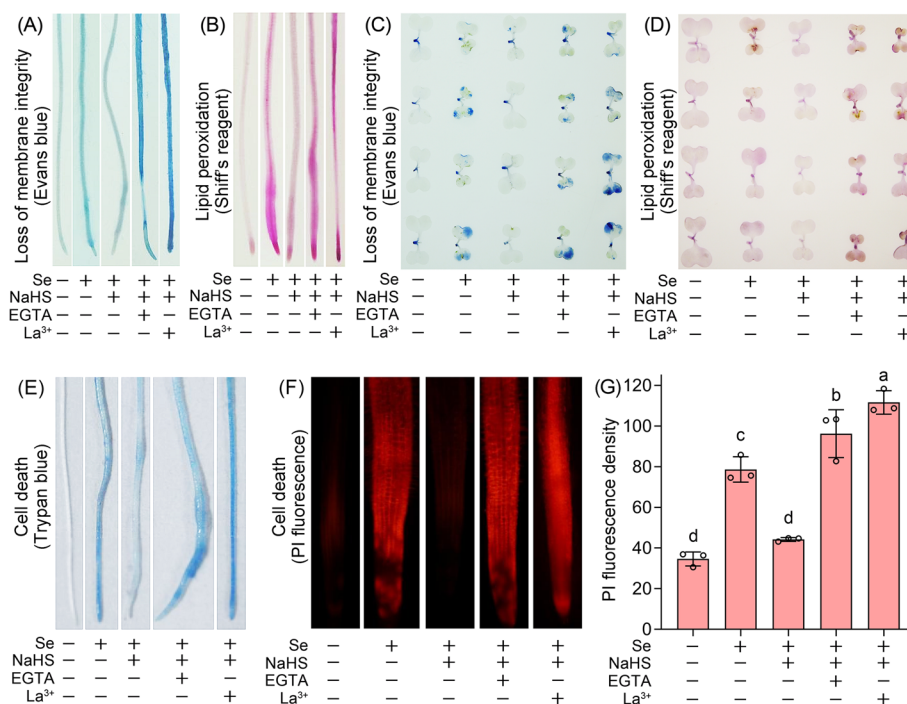


Fig. 10 H₂S-Ca²⁺ interaction attenuated oxidative injury and cell death in *B. rapa* upon Se stress. **A** Loss of membrane integrity in roots upon NaHS, EGTA (0.5 mM), or La³⁺ (50 μM) in the presence of Se (20 μM) for 72 h. **B** Lipid peroxidation in roots. **C** Loss of membrane integrity in leaves. **D** Lipid peroxidation in leaves. **E** Root cell death stained by Trypan blue. **F** Root cell death indicated by PI fluorescence. **G** Calculated PI fluorescent density. Different lowercase letters in (G) indicated significant difference among different treatments (n = 3; P < 0.05; LSD)

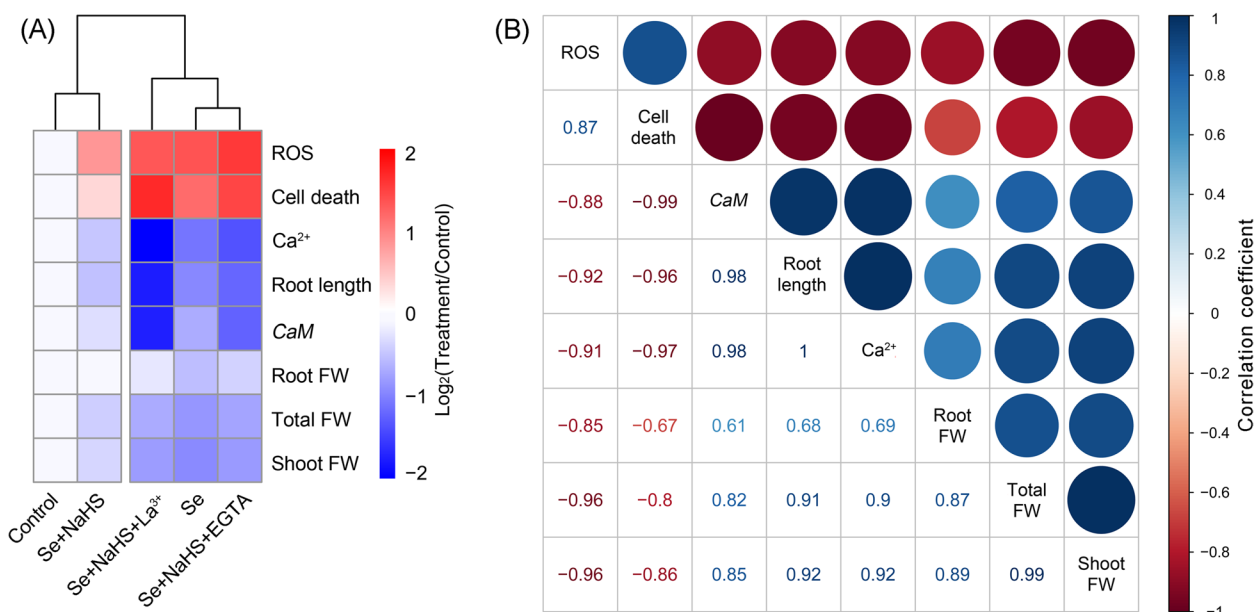


Fig. 11 Cluster analysis of H₂S-Ca²⁺-facilitated Se tolerance in *B. rapa*. **A** Hierarchical cluster analysis among different treatments based on obtained physiological parameters. The legend showed the value of Log₂(Treatment/Control) for each parameter. Red, white, and blue indicated upregulation, unchanged, and downregulation, respectively, for each treatment as compared to control. **B** Pearson correlation analysis among different physiological parameters under the same treatment setup (Control, Se, Se + NaHS, Se + NaHS + EGTA, and Se + NaHS + La³⁺)

concentration more than 5 μM inhibited the growth of *B. rapa* seedlings, with 20 μM of Se resulted in moderate inhibition of seedling growth. Se-induced phytotoxicity not only depends on plant species, but also depends on the growth stage of plant. Further studies are needed to identify the toxic dose of Se on adult plants of *B. rapa*.

We previously found that endogenous H_2S is vital for the survival of *B. rapa* seedlings under Se stress (Chen et al. 2014b). In this study, four lines of evidence indicate that H_2S - Ca^{2+} interaction plays a role in combating Se stress in *B. rapa*. First, Se stress inhibited the growth of *B. rapa* by inducing oxidative stress. Second, the biosynthesis of endogenous H_2S in *B. rapa* was suppressed at the end of Se exposure. Enhancing endogenous H_2S alleviated growth inhibition of *B. rapa* under Se stress, an effect reversed by decreasing endogenous H_2S . Third, Se stress decreased endogenous Ca^{2+} level and *BrCaMI* expression in *B. rapa*, which were elevated by enhancing endogenous H_2S . Fourth, H_2S -ameliorated oxidative stress and growth inhibition were blocked by decreasing endogenous Ca^{2+} in *B. rapa* under Se stress. These results suggested that H_2S conferred Se tolerance by regulating Ca^{2+} signaling in *B. rapa*.

Excessive Se frequently induce oxidative injury in plants (Hasanuzzaman et al. 2020a; Van Hoewyk 2013). The antioxidative role of H_2S has been widely identified in plants (Liu et al. 2021; Zhang et al. 2021). We found increased endogenous H_2S in *B. rapa* at early stage of Se exposure, suggesting that Se stress triggered H_2S -mediated defensive responses. However, prolonged exposure of Se led to decreased endogenous H_2S , accompanying the occurrence of oxidative injury and growth inhibition. Se stress for 72 h finally dampens the defensive role of H_2S , leading to phytotoxicity. NaHS is a reliable donor of H_2S for suppressing ROS in roots (Chen et al. 2014b). NaHS-provided H_2S enhanced endogenous H_2S level in Se-treated roots up to 72 h, leading to the detoxification of excessive Se by alleviating oxidative stress in *B. rapa*. These results propose a defensive role of endogenous H_2S against Se stress.

The expression patterns of *BrLCDs* and *BrDCDs* were similar to the changes of endogenous H_2S level in *B. rapa* under Se stress. This suggested that Se stress disturbed the biosynthesis of endogenous H_2S . The H_2S biosynthesis can be differentially regulated by different environmental stimuli. Cadmium stress induces H_2S biosynthesis by activating both LCD and DCD in alfalfa (Cui et al. 2014). Drought stress triggers the expression of LCD but not DCD in *Arabidopsis thaliana* (Shen et al. 2013). The gene expression is mainly controlled by the cis-elements in the promoter region of the gene. Se stress may regulate gene promoters to modulate gene expression in plants (Chen et al. 2014a). Further studies are needed to identify

the cis-elements in the promoters of *LCDs* and *DCDs*. This may help understand the differential regulation of plant H_2S biosynthesis by Se stress and other environmental stimuli.

Ca^{2+} is a universal messenger regulating plant stress responses (Pirayesh et al. 2021). Little is known about the role of Ca^{2+} in the regulation of Se-induced phytotoxicity. In this study, H_2S -promoted Ca^{2+} was associated with the growth promotion of *B. rapa* under Se stress. H_2S triggered intracellular Ca^{2+} signaling that further attenuated oxidative stress and growth inhibition in *B. rapa* under Se stress. The cross-talk between H_2S and Ca^{2+} play a role in alleviating oxidative damage in plants upon abiotic stresses. Ca^{2+} interacts with H_2S can ameliorate oxidative injury to confer salt tolerance in mung bean roots (Khan et al. 2021). The interplay between H_2S and Ca^{2+} /*CaM* facilitates acclimation of zucchini to nickel toxicity by suppressing oxidative stress (Valivand et al. 2019). Having link Ca^{2+} and H_2S into a signaling cassette provides new signaling events of Se tolerance in plants. In mammalian cells, H_2S interacts with the sulfhydryl group of Ca^{2+} channel protein to regulate its activity, leading to the modulation of Ca^{2+} homeostasis (Munaron et al. 2013; Yong et al. 2010). The Ca^{2+} channel blocker compromised H_2S -conferred tolerance against Se stress, suggesting the possible role of Ca^{2+} channel in H_2S signaling. Further studies are needed to identify the possible target Ca^{2+} channel that can be regulated H_2S in plants upon Se stress.

The interaction between H_2S and Ca^{2+} /*CaM* has been found in both plants and fungi. H_2S improves heat tolerance of tobacco by triggering the influx of extracellular Ca^{2+} into cytosol, working with *CaM* (Li et al. 2012). H_2S induces betulin accumulation by elevating endogenous Ca^{2+} and *CaM* in the mycelia of *Phellinus linteus* (Fan et al. 2016). Ca^{2+} can also work upstream of H_2S . In *Arabidopsis* against chromium stress, Ca^{2+} /*CaM2* interacts with transcription factor TGA3 to facilitate the binding of TGA3 to the promoter of *LCD*, enhancing the transcription of *LCD* to promote H_2S generation (Fang et al. 2017). In the present study, Ca^{2+} /*CaM* acts downstream of H_2S to improve Se tolerance in *B. rapa*. Whether and how Ca^{2+} modulates H_2S signaling through a possible feedback regulation need further investigation.

Se is an essential micronutrient for both crops and humans. It is important to avoid Se pollution during Se biofortification performance to achieve the development of sustainable agriculture. In Se-deficient areas, efforts are made to enhance the uptake and assimilation of Se in crops. This can be achieved by supplying organic Se fertilizers at low level because crops prefer to accumulate organic forms of Se. This would help minimize the overaccumulation of exogenous Se in agricultural

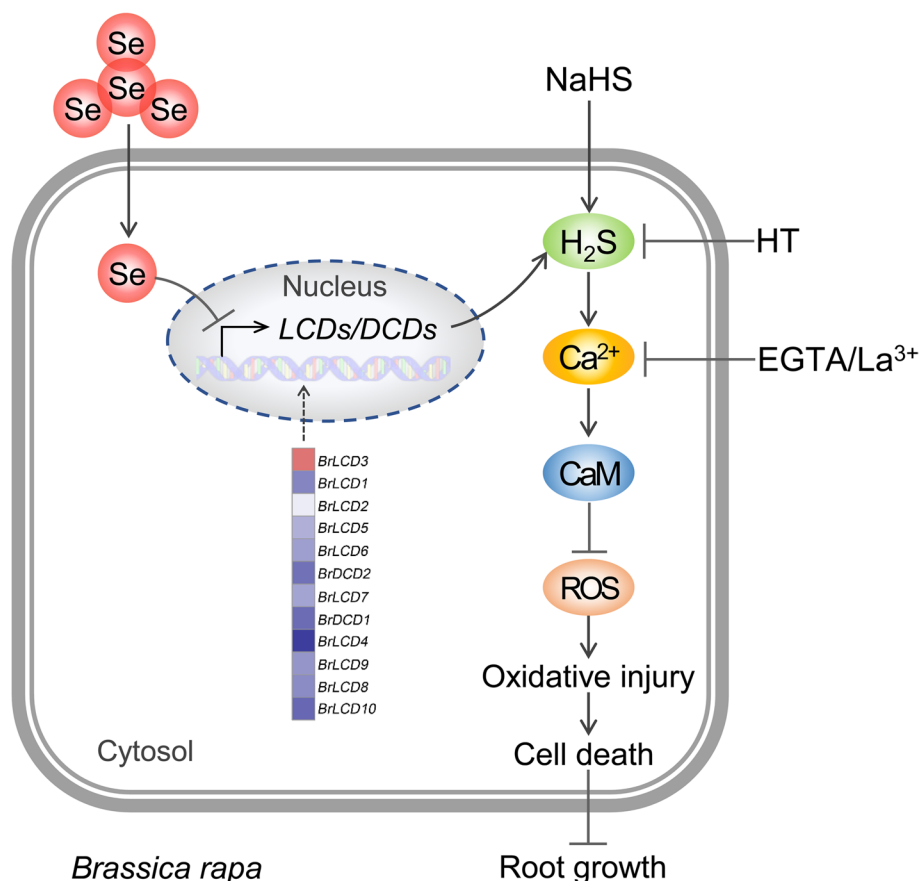


Fig. 12 Schematic model of the role of H₂S-Ca²⁺ interaction in the regulation of Se tolerance in *B. rapa*. Se exposure decreases endogenous H₂S level by downregulating the expression of LCDs and DCDs. NaHS-provided H₂S enhances endogenous H₂S level upon Se stress. Elevated H₂S triggers Ca²⁺/CaM signaling to alleviate ROS accumulation, oxidative injury and cell death, further promoting root growth. The beneficial effect of NaHS can be abolished by adding HT, EGTA, or La³⁺. NaHS, H₂S donor; HT, H₂S scavenger; EGTA, Ca²⁺ chelator; La³⁺, influx channel blocker

environment. Another possible approach is the genetic engineering of crops with enhanced Se uptake ability (Malagoli et al. 2015). In Se-polluted areas, phytoremediation is a promising approach to decrease Se level in soil. The byproducts of Se phytoremediation need to be disposed carefully (Hasanuzzaman et al. 2020b; Zhu et al. 2009). It is also possible to promote crop tolerance against Se stress in Se-polluted soil. In the present study, exogenous application of H₂S donor was able to trigger Se tolerance in *B. rapa*, but it is difficult to apply H₂S in field because of the inevitable loss of gaseous H₂S. The promising approach is to construct nano-emulsion particles to package donors, achieving the sustainable supply of gaseous molecules for a long time (Wang et al. 2021b).

Conclusion

Understanding plant physiological adaptation to Se stress is important for the management of excessive Se pollution. This study revealed a new signaling module (H₂S-Ca²⁺) involved in plant response to Se stress.

Ca²⁺/CaM acts as a downstream player of H₂S to facilitate plant tolerance against Se stress. H₂S, Ca²⁺ and CaM worked as a linear signaling cassette to suppress ROS accumulation followed by the alleviation of oxidative injury and cell death, promoting root growth under Se stress (Fig. 12). More evidences are needed to identify the detailed biochemical mechanisms for H₂S-Ca²⁺ interaction in Se-treated plants, but our current results would help understand the adaptation of plants to Se contamination.

Abbreviations

CaM	Calmodulin
DAB	3,3-Diaminobenzidine
DCD	γ-cysteine desulfhydrase
DCF	2',7'-Dichlorofluorescein
EGTA	Ethylene glycol-bis(2-aminoethylether)-N,N,N',N'-tetraacetic acid
H ₂ S	Hydrogen sulfide
HT	Hypotaourine
LCD	L-cysteine desulfhydrase
NBT	Nitro-blue tetrazolium
PI	Propidium iodide

RNS	Reactive nitrogen species
ROS	Reactive oxygen species
Se	Selenium
WSP-1	Washington State Probe-1

Supplementary Information

The online version contains supplementary material available at <https://doi.org/10.1186/s43014-023-00207-3>.

Additional file 1: Table S1. Sequences of primers used for qRT-PCR analysis.

Acknowledgements

We appreciate Mr. Cunfa Xu from Central Laboratory in Jiangsu Academy of Agricultural Sciences for microscopic assistance.

Authors' contributions

Lifei Yang and Jian Chen conceptualized and designed the study. Xiefeng Ye and Haiyan Lu designed the experiments. Xiefeng Ye and Haiyan Lu finished phenotypic and histochemical analysis. Aijing Xin finished gene expression analysis. Ruixian Liu and Zhiqi Shi finished fluorescent detection and analyzed the data. Xiefeng Ye, Haiyang Lu, and Aijing Xin wrote the original draft. Lifei Yang and Jian Chen reviewed and edited the draft.

Funding

This research was funded by National Natural Science Foundation of China (32071968), China Agriculture Research System (CARS-23-B16), and Jiangsu Agricultural Science and Technology Innovation Fund [CX(20)1011].

Availability of data and materials

All data generated or analysed during this study are included in this published article and its supplementary information files.

Declarations

Ethics approval and consent to participate

Not applicable.

Consent for publication

Not applicable.

Competing interests

The authors declare no conflict of interest.

Author details

¹National Tobacco Cultivation and Physiology and Biochemistry Research Centre, Key Laboratory for Tobacco Cultivation of Tobacco Industry, Tobacco Science College, Henan Agricultural University, Zhengzhou 450002, China. ²Laboratory for Food Quality and Safety-State Key Laboratory Cultivation Base of Ministry of Science and Technology, Institute of Food Safety and Nutrition, Jiangsu Academy of Agricultural Sciences, Nanjing 210014, China. ³College of Horticulture, Hexian New Countryside Development Research Institute, Nanjing Agricultural University, Nanjing 210095, China. ⁴Institute of Industrial Crops, Provincial Key Laboratory of Agrobiolgy, Jiangsu Academy of Agricultural Sciences, Nanjing 210014, China.

Received: 7 August 2023 Accepted: 5 November 2023

Published online: 03 June 2024

References

- Akbulut, M., & Cakir, S. (2010). The effects of Se phytotoxicity on the antioxidant systems of leaf tissues in barley (*Hordeum vulgare* L.) seedlings. *Plant Physiology and Biochemistry*, *48*(2–3), 160–166.
- Arif, Y., Hayat, S., Yusuf, M., & Bajguz, A. (2021). Hydrogen sulfide: a versatile gaseous molecule in plants. *Plant Physiology and Biochemistry*, *158*, 372–384.
- Bajaj, M., Eiche, E., Neumann, T., Winter, J., & Gallert, C. (2011). Hazardous concentrations of selenium in soil and groundwater in North-West India. *Journal of Hazardous Materials*, *189*(3), 640–646.
- Chen, C., Chen, H., Zhang, Y., Thomas, H. R., Frank, M. H., He, Y., & Xia, R. (2020). TBtools: an integrative toolkit developed for interactive analyses of big biological data. *Molecular Plant*, *13*(8), 1194–1202.
- Chen, Y., Mo, H. Z., Hu, L., Li, Y., Chen, J., & Yang, L. (2014a). The endogenous nitric oxide mediates selenium-induced phytotoxicity by promoting ROS generation in *Brassica rapa*. *PLoS One*, *9*(10), e110901.
- Chen, Y., Mo, H. Z., Zheng, M. Y., Xian, M., Qi, Z. Q., Li, Y. Q., Hu, L. B., Chen, J., & Yang, L. F. (2014). Selenium inhibits root elongation by repressing the generation of endogenous hydrogen sulfide in *Brassica rapa*. *PLoS One*, *9*(10), e110904.
- Cheng, Y., Wang, N., Liu, R., Bai, H., Tao, W., Chen, J., & Shi, Z. (2021). Cinnamaldehyde facilitates cadmium tolerance by modulating Ca²⁺ in *Brassica rapa*. *Water Air & Soil Pollution*, *232*(1), 19.
- Cui, W., Chen, H., Zhu, K., Jin, Q., Xie, Y., Cui, J., Xia, Y., Zhang, J., & Shen, W. (2014). Cadmium-induced hydrogen sulfide synthesis is involved in cadmium tolerance in *Medicago sativa* by reestablishment of reduced (Homo)glutathione and reactive oxygen species homeostases. *PLoS One*, *9*(10), e109669.
- Etteieb, S., Magdoui, S., Zolfaghari, M., & Brar, S. (2020). Monitoring and analysis of selenium as an emerging contaminant in mining industry: a critical review. *Science of the Total Environment*, *698*, 134339.
- Fan, G., Jian, D., Sun, M., Zhan, Y., & Sun, F. (2016). Endogenous and exogenous calcium involved in the betulin production from submerged culture of *Phellinus linteus* induced by hydrogen sulfide. *Applied Biochemistry and Biotechnology*, *178*(3), 594–603.
- Fang, H., Jing, T., Liu, Z., Zhang, L., Jin, Z., & Pei, Y. (2014). Hydrogen sulfide interacts with calcium signaling to enhance the chromium tolerance in *Setaria italica*. *Cell Calcium*, *56*(6), 472–481.
- Fang, H., Liu, Z., Long, Y., Liang, Y., Jin, Z., Zhang, L., Liu, D., Li, H., Zhai, J., & Pei, Y. (2017). The Ca²⁺/calmodulin2-binding transcription factor TGA3 elevates LCD expression and H₂S production to bolster Cr⁶⁺ tolerance in Arabidopsis. *The Plant Journal*, *91*(6), 1038–1050.
- Hasanuzzaman, M., Bhuyan, M. H. M. B., Raza, A., Hawrylak-Nowak, B., Matraszek-Gawron, R., Mahmud, J. A., Nahar, K., & Fujita, M. (2020). Selenium in plants: Boon or bane? *Environmental and Experimental Botany*, *178*, 104170.
- Hasanuzzaman, M., Bhuyan, M. H. M. B., Raza, A., Hawrylak-Nowak, B., Matraszek-Gawron, R., Nahar, K., & Fujita, M. (2020). Selenium toxicity in plants and environment: biogeochemistry and remediation possibilities. *Plants*, *9*(12), 1711.
- Hawrylak-Nowak, B. (2008). Changes in anthocyanin content as indicator of maize sensitivity to selenium. *Journal of Plant Nutrition*, *31*(7), 1232–1242.
- Hawrylak-Nowak, B. (2013). Comparative effects of selenite and selenate on growth and selenium accumulation in lettuce plants under hydroponic conditions. *Plant Growth Regulation*, *70*, 149–157.
- Hawrylak-Nowak, B., Matraszek, R., & Pogorzelec, M. (2015). The dual effects of two inorganic selenium forms on the growth, selected physiological parameters and macronutrients accumulation in cucumber plants. *Acta Physiologiae Plantarum*, *37*, 41.
- He, Y., Xiang, Y., Zhou, Y., Yang, Y., Zhang, J., Huang, H., Shang, C., Luo, L., Gao, J., & Tang, L. (2018). Selenium contamination, consequences and remediation techniques in water and soils: A review. *Environmental Research*, *164*, 288–301.
- Huang, S., Hua, M., Feng, J., Zhong, X., Jin, Y., Zhu, B., & Lu, H. (2009). Assessment of selenium pollution in agricultural soils in the Xuzhou District, Northwest Jiangsu, China. *Journal of Environmental Sciences*, *21*(4), 481–487.
- Kausch, M. F., & Pallud, C. E. (2013). Science, policy, and management of irrigation-induced selenium contamination in California. *Journal of Environmental Quality*, *42*(6), 1605–1614.
- Khan, M. N., Siddiqui, M. H., Mukherjee, S., Alamri, S., Al-Amri, A. A., Alsubaie, Q. D., Al-Munqedhi, B. M. A., & Ali, H. M. (2021). Calcium-hydrogen sulfide crosstalk during K⁺-deficient NaCl stress operates through regulation of Na⁺/H⁺ antiport and antioxidative defense system in mung bean roots. *Plant Physiology and Biochemistry*, *159*, 211–225.
- Kolbert, Z., Lehotai, N., Molnar, A., & Feigl, G. (2016). The roots of selenium toxicity: a new concept. *Plant Signaling and Behavior*, *11*(10), e1241935.

- Kuisi, M. A., & Abdel-Fattah, A. (2010). Groundwater vulnerability to selenium in semi-arid environments: Amman Zarqa Basin, Jordan. *Environmental Geochemistry and Health*, 32(2), 107–128.
- Łabanowska, M., Filek, M., Kościelniak, J., Kurdziel, M., Kuliś, E., & Hartikainen, H. (2012). The effects of short-term selenium stress on Polish and Finnish wheat seedlings-EPR, enzymatic and fluorescence studies. *Journal of Plant Physiology*, 169(3), 275–284.
- Lehotai, N., Lyubenova, L., Schröder, P., Feigl, G., Ördög, A., Szilágyi, K., Erdei, L., & Kolbert, Z. (2016). Nitro-oxidative stress contributes to selenite toxicity in pea (*Pisum sativum* L.). *Plant and Soil*, 400(1), 107–122.
- Li, Y. J., Chen, J., Xian, M., Zhou, L. G., Han, F. X., Gan, L. J., & Shi, Z. Q. (2014). *In site* bioimaging of hydrogen sulfide uncovers its pivotal role in regulating nitric oxide-induced lateral root formation. *PLoS One*, 9(2), e90340.
- Li, Z. G. (2019). Interplay between hydrogen sulfide and calcium signaling in plant abiotic stress response and adaptation. In M. Hasanuzzaman, V. Fotopoulos, K. Nahar, & M. Fujita (Eds.), *Reactive oxygen, nitrogen and sulfur species in plants* (pp. 669–683). Wiley-Blackwell.
- Li, Z. G., Gong, M., Xie, H., Yang, L., & Li, J. (2012). Hydrogen sulfide donor sodium hydrosulfide-induced heat tolerance in Tobacco (*Nicotiana tabacum* L.) suspension cultured cells and involvement of Ca²⁺ and calmodulin. *Plant Science*, 185–186(0), 185–189.
- Liu, H., Wang, J., Liu, J., Liu, T., & Xue, S. (2021). Hydrogen sulfide (H₂S) signaling in plant development and stress responses. *ABIOTECH*, 2(1), 32–63.
- Livak, K. J., & Schmittgen, T. D. (2001). Analysis of relative gene expression data using real-time quantitative PCR and the 2^{-ΔΔCT} method. *Methods*, 25(4), 402–408.
- Lyons, G. H., Stangoulis, J. C. R., & Graham, R. D. (2005). Tolerance of wheat (*Triticum aestivum* L.) to high soil and solution selenium levels. *Plant and Soil*, 270(1), 179–188.
- Malagoli, M., Schiavon, M., dall'Acqua, S., & Pilon-Smits, E. A. H. (2015). Effects of selenium biofortification on crop nutritional quality. *Frontiers in Plant Science*, 6, 280.
- Mehdi, Y., Hornick, J. L., Istasse, L., & Dufrasne, I. (2013). Selenium in the environment, metabolism and involvement in body functions. *Molecules*, 18(3), 3292–3311.
- Molnár, Á., Kolbert, Z., Kéri, K., Feigl, G., Ördög, A., Szöllösi, R., & Erdei, L. (2018). Selenite-induced nitro-oxidative stress processes in *Arabidopsis thaliana* and *Brassica juncea*. *Ecotoxicology and Environmental Safety*, 148, 664–674.
- Munaron, L., Avanzato, D., Moccia, F., & Mancardi, D. (2013). Hydrogen sulfide as a regulator of calcium channels. *Cell Calcium*, 53(2), 77–84.
- Pirayesh, N., Giridhar, M., Ben Khedher, A., Vothknecht, U. C., & Chigri, F. (2021). Organellar calcium signaling in plants: an update. *Biochimica et Biophysica Acta Molecular Cell Research*, 1868(4), 118948.
- Sakamoto, M., Chan, M., Domingo, H., Kubota, J. L., & Murata, K. (2012). Changes in body burden of mercury, lead, arsenic, cadmium and selenium in infants during early lactation in comparison with placental transfer. *Ecotoxicology and Environmental Safety*, 84, 179–184.
- Sarwar, N., Akhtar, M., Kamran, M. A., Imran, M., Riaz, M. A., Kamran, K., & Hussain, S. (2020). Selenium biofortification in food crops: key mechanisms and future perspectives. *Journal of Food Composition and Analysis*, 93, 103615.
- Shen, J., Xing, T., Yuan, H., Liu, Z., Jin, Z., Zhang, L., & Pei, Y. (2013). Hydrogen sulfide improves drought tolerance in *Arabidopsis thaliana* by microRNA expressions. *PLoS One*, 8(10), e77047.
- Tong, T., Li, Q., Jiang, W., Chen, G., Xue, D., Deng, F., Zeng, F., & Chen, Z. H. (2021). Molecular evolution of calcium signaling and transport in plant adaptation to abiotic stress. *International Journal of Molecular Sciences*, 22(22), 12308.
- Valivand, M., Amooaghaie, R., & Ahadi, A. (2019). Interplay between hydrogen sulfide and calcium/calmodulin enhances systemic acquired acclimation and antioxidative defense against nickel toxicity in zucchini. *Environmental and Experimental Botany*, 158, 40–50.
- Van Hoewyk, D. (2013). A tale of two toxicities: Malformed selenoproteins and oxidative stress both contribute to selenium stress in plants. *Annals of Botany*, 112(6), 965–972.
- Vinceti, M., Crespi, C. M., Bonvicini, F., Malagoli, C., Ferrante, M., Marmioli, S., & Stranges, S. (2013). The need for a reassessment of the safe upper limit of selenium in drinking water. *Science of the Total Environment*, 443, 633–642.
- Wang, C., Deng, Y., Liu, Z., & Liao, W. (2021). Hydrogen sulfide in plants: crosstalk with other signal molecules in response to abiotic stresses. *International Journal of Molecular Sciences*, 22(21), 12068.
- Wang, Y., Lv, P., Kong, L., Shen, W., & He, Q. (2021). Nanomaterial-mediated sustainable hydrogen supply induces lateral root formation via nitrate reductase-dependent nitric oxide. *Chemical Engineering Journal*, 405, 126905.
- Winkel, L. H. E., Johnson, C. A., Lenz, M., Grundl, T., Leupin, O. X., Amini, M., & Charlet, L. (2012). Environmental selenium research: From microscopic processes to global understanding. *Environmental Science & Technology*, 46(2), 571–579.
- Yang, L., Yang, H., Bian, Z., Lu, H., Zhang, L., & Chen, J. (2022). The defensive role of endogenous H₂S in *Brassica rapa* against mercury-selenium combined stress. *International Journal of Molecular Sciences*, 23(5), 2854.
- Ye, X., Ling, T., Xue, Y., Xu, C., Zhou, W., Hu, L., Chen, J., & Shi, Z. (2016). Thymol mitigates cadmium stress by regulating glutathione levels and reactive oxygen species homeostasis in tobacco seedlings. *Molecules*, 21(10), 1339.
- Yong, Q. C., Choo, C. H., Tan, B. H., Low, C. M., & Bian, J. S. (2010). Effect of hydrogen sulfide on intracellular calcium homeostasis in neuronal cells. *Neurochemistry International*, 56(3), 508–515.
- Zelmanov, G., & Semiat, R. (2013). Selenium removal from water and its recovery using iron (Fe³⁺) oxide/hydroxide-based nanoparticles sol (NanoFe) as an adsorbent. *Separation and Purification Technology*, 103, 167–172.
- Zhang, J., Zhou, M., Zhou, H., Zhao, D., Gotor, C., Romero, L. C., Shen, J., Ge, Z., Zhang, Z., Shen, W., Yuan, X., & Xie, Y. (2021). Hydrogen sulfide, a signaling molecule in plant stress responses. *Journal of Integrative Plant Biology*, 63(1), 146–160.
- Zhou, Z. S., Wang, S. J., & Yang, Z. M. (2008). Biological detection and analysis of mercury toxicity to alfalfa (*Medicago sativa*) plants. *Chemosphere*, 70(8), 1500–1509.
- Zhu, Y. G., Pilon-Smits, E. A., Zhao, F. J., Williams, P. N., & Meharg, A. A. (2009). Selenium in higher plants: Understanding mechanisms for biofortification and phytoremediation. *Trends in Plant Science*, 14(8), 436–442.

Publisher's Note

Springer Nature remains neutral with regard to jurisdictional claims in published maps and institutional affiliations.

Ready to submit your research? Choose BMC and benefit from:

- fast, convenient online submission
- thorough peer review by experienced researchers in your field
- rapid publication on acceptance
- support for research data, including large and complex data types
- gold Open Access which fosters wider collaboration and increased citations
- maximum visibility for your research: over 100M website views per year

At BMC, research is always in progress.

Learn more biomedcentral.com/submissions

